Published in final edited form as:
Nucl Med Biol. 2013 January ; 40(1): 52–59. doi:10.1016/j.nucmedbio.2012.08.008.

Targeting Breast Carcinoma with Radioiodinated Anti-HER2 Nanobody

Marek Pruszynski[a], **Eftychia Koumarianou**[a], **Ganesan Vaidyanathan**[a], **Hilde Revets**[c], **Nick Devoogdt**[d], **Tony Lahoutte**[d], and **Michael R. Zalutsky**[a,b,*]

[a]Department of Radiology, Duke University Medical Center, Durham, NC 27710, USA

[b]Department of Radiation Oncology, Duke University Medical Center, Durham, NC 27710, USA

[c]Ablynx nv, Ghent 9052, Belgium

[d]In Vivo Cellular and Molecular Imaging, Vrije Universiteit Brussel, Brussels, Belgium

Abstract

Introduction—With a molecular weight an order of magnitude lower than antibodies but possessing comparable affinities, Nanobodies (Nbs) are attractive as targeting agents for cancer diagnosis and therapy. An anti-HER2 Nb could be utilized to determine HER2 status in breast cancer patients prior to trastuzumab treatment. This provided motivation for the generation of HER2-specific 5F7GGC Nb, its radioiodination and evaluation for targeting HER2 expressing tumors.

Methods—5F7GGCNb was radioiodinated with ^{125}I using Iodogen and with ^{131}I using the residualizing agent N^{ε}-(3-[^{131}I]iodobenzoyl)-Lys^{5}-N$^{\alpha}$-maleimido-Gly^{1}-GEEEK ([^{131}I]IB-Mal-D-GEEEK) used previously successfully with intact antibodies. Paired-label internalization assays using BT474M1 cells and tissue distribution experiments in athymic mice bearing BT474M1 xenografts were performed to compare the two labeled Nb preparations.

Results—The radiochemical yields for Iodogen and [^{131}I]IB-Mal-D-GEEEK labeling were 83.6±5.0%(n= 10) and 59.6±9.4% (n = 15), respectively. The immunoreactivity of labeled proteins was preserved as confirmed by *in vitro* and *in vivo* binding to tumor cells. Biodistribution studies showed that Nb radiolabeled using [^{131}I]IB-Mal-D-GEEEK, compared with the directly labeled Nb, had a higher tumor uptake (4.65 ± 0.61% ID/g vs. 2.92 ± 0.24% ID/g at 8 h), faster blood clearance, lower accumulation in non-target organs except kidneys, and as a result, higher concomitant tumor-to-blood and tumor-to-tissue ratios.

Conclusions—Taken together, these results demonstrate that 5F7GGC anti-HER2 Nb labeled with residualizing [^{131}I]IB-Mal-D-GEEEK had better tumor targeting properties compared to the directly labeled Nb suggesting the potential utility of this Nb conjugate for SPECT (^{123}I)and PET imaging (^{124}I) of patients with HER2-expressing tumors.

Keywords

HER2; Nanobody; breast cancer; VHH; radioiodination; IB-Mal-D-GEEEK

*Corresponding author. Tel.: +1 919 684 7708; fax: +1 919 684 7121. zalut001@mc.duke.edu (M.R. Zalutsky).

1. Introduction

Human epidermal growth factor receptor 2 (HER2) is a 185 kDa transmembrane protein that belongs to the HER family of tyrosine kinase receptors [1]. HER2 overexpression occurs in about 20–30% of breast cancers, 4–6% of non-small cell lung cancers, 20–24% of gastric cancers, as well as in colon and ovarian cancers[2–4]. Trastuzumab (Herceptin®, Genentech)is a humanized IgG1 monoclonal antibody (mAb) currently used to treat patients with HER2-positive malignancies[4–6]. Because patients with low and/or heterogeneous HER2 expression have a poorer response to trastuzumab treatment [7],, determination of HER2 status is essential in selecting patients for trastuzumab therapy. Molecular imaging is an attractive approach for accomplishing this task; however, using full-size monoclonal antibodies (mAbs) like trastuzumab for imaging is not ideal because of their long residence time in blood.

Nanobodies (Nbs), also referred to as single domain antibodies or VHH molecules, are proteins based on the smallest functional fragments of heavy chain antibodies, and naturally occur in *Camelidae*. With a molecular weight of 12–15 kDa, Nbs are an order of magnitude smaller than intact mAbs, and smaller than Fab (~50 kDa) and scFv (~25 kDa)fragments [8]. Their small size and nanomolar-range affinities make them very attractive for tumor targeting applications. Moreover, Nbs exhibit high thermal and chemical stability, and compared with intact mAbs and their fragments, are less lipophilic, more water-soluble and have a lower tendency for aggregation [9]. Specific Nbs against enzymes, haptens, pathogens, toxins and tumor markers have been generated [9–11]. For these reasons, Nbs are an attractive platform for radiolabeling and application as cancer imaging agents.

With regard to radiolabeling, previous studies have shown that the cumulative radioactivity retained by tumor from directly radioiodinated mAbs that bind to internalizing targets such as HER2 is compromised by the rapid efflux of labeled iodotyrosine resulting from the degradation of the labeled mAb within the lysosomes [12,13]. To circumvent this problem, we have developed several radio halogenation approaches for internalizing mAbs that augment the retention of radioactivity in tumor cells after intracellular processing [14–16]. Perhaps the most promising tactic for intact mAbs has been to couple them to radiolabeled D-amino acid peptides that are positively or negatively charged at lysosomal pH[17–20]. The IB-Mal-D-GEEEK reagent, which contains multiple negatively charged D-amino acids, has been particularly effective in enhancing the retention of radioactivity in tumor cells and xenografts after receptor-mediated internalization of labeled mAbs[19,20].

In the current study, we describe the generation and production of Nb 5F7GGC, which binds specifically to HER2. The Nb was radioiodinated using both a conventional method (Iodogen) as well as with the IB-Mal-D-GEEEK reagent, and tumor targeting properties of the labeled Nbs were compared *in* vitro and *in vivo*.

2. Materials and methods

2.1. General

All reagent grade chemicals were purchased from Sigma-Aldrichunless otherwise specified, and used as received. Sodium [^{125}I]iodide and sodium [^{131}I]iodide in 0.1N NaOH with specific activities of 650 GBq/mg and 550 GBq/mg, respectively, were purchased from Perkin-Elmer Life and Analytical Sciences (Boston, MA, USA). HPLC was performed using a Beckman Gold system equipped with a Model 126 programmable solvent module coupled with UV (Model 168 diode array) and radiometric (Gamma Detector 170) detectors, and a Beckman System Gold SS420X remote interface system; the data were acquired using 32 Karat software. For reversed-phase HPLC, a WatersC18 column (XTerra C18; 5 μm, 250

× 4.5 mm) was used. Solvents for HPLC were obtained as HPLC grade and degassed by ultrasonication for 15–20 min just before use. The synthesis of tin precursor N^{ε}-(3-(tri-n-butyltin)benzoyl)-Lys^{5}-N$^{\alpha}$-maleimido-Gly^{1}-D-GEEEK(TB-Mal-D-GEEEK)and its use for radioiodination were performed as reported before[19]. All reagents used in cell culture studies were purchased from Invitrogen (Grand Island, NY, USA) except where noted. Trastuzumab (Herceptin®) was obtained from Genentech (San Francisco, CA, USA).

2.2 Nanobody

2.2.1 Selection and characterization of anti-HER2 Nanobody 5F7—The anti-HER2 Nanobody® (Ablynx registered trademark for Nb)5F7 was generated using phage display at Ablynx NV (Ghent, Belgium) using established protocols as described [21]. Briefly, phage libraries were constructed from peripheral blood mononuclear cells derived from llamas immunized with SKBR3 human breast carcinoma cells, a cell line derived from an adenocarcinoma overexpressing HER2 p185 tyrosine kinase (SKBR3; ATCC HTB-30). Phage libraries were then incubated on immobilized ErbB2/Fc chimera (R&D Systems, Minneapolis, MN, USA) and after extensive washing, bound phage were specifically eluted with trastuzumab. Eluted phage were rescued via infection of *E. coli*. Individual colonies were picked and grown in 96 deep well plates (1 ml). Nb expression was induced by addition of isopropyl β-D-1-thiogalactopyranoside (IPTG) and periplasmic extracts (80 μl) were prepared according to standard methods. Alternatively, selected Nbs were expressed in the periplasmic space of *E. coli* as c-myc, His_6 tagged proteins in a culture volume of 50 ml and purified via immobilized metal affinity chromatography (IMAC). Nbs were eluted from the column with 250 mM imidazole followed by gel filtration and buffer exchange to PBS.

To determine whether Nbs recognized cell-surface expressed HER2, binding to SKBR3 cells was assessed by flow cytometry. Cell binding assays were carried out by incubating SKBR3 cells with Nb-containing periplasmic preparations obtained from 96 deep well cultures. After incubation, the cells were washed with fluorescence-activated cell sorting (FACS) buffer and subsequently incubated successively with mouse anti-myc-tag mAb (9E10 clone) and phycoerythrin labeled goat anti-mouse $F(ab')_2$ fragments (Jackson ImmunoResearch). Cells were finally analyzed on a BD FACS Array Bioanalyzer System (BD Biosciences).

Nbs were also screened in a trastuzumab-competitive homogeneous cell-based assay to evaluate the capacity of the expressed Nbs to block trastuzumab binding to HER2. The fluorometric micro volume assay technology (FMAT) 8200 HTS system (Applied Biosystems, Foster City, CA, USA) assay was performed as follows: serial dilutions of purified Nb (concentration range: 20 nM – 10 pM) were added to SKBR3 cells together with 4×10^{-10} MAlexa647-labeled trastuzumab and incubated for 2 h, after which plates were scanned. Trastuzumab was included as a reference mAb.

2.2.2 Measurement of Nanobody-antigen binding kinetics and K_D—Kinetic (ka and kd) and dissociation(K_D) constants of purified Nb 5F7 were determined at Ablynxby surface plasmon resonance on a Biacore T100 instrument. Approximately 740 RU of rhErbB2/Fc was immobilized on a CM5 sensor chip surface. Nb binding was assessed at varying concentrations ranging from 15–500 nM. The samples were injected for 1 min at a flow rate of 45μl/min to allow for binding to chip-bound antigen. Next, binding buffer without Nb was sent over the chip at the same flow rate to allow dissociation of bound Nb. After 10 min, any remaining bound analyte was removed by injecting regeneration solution (1M NaCl, 50mM NaOH). Binding/dissociation curves were used to calculate K_D values.

2.2.3 Production and purification of cysteine-tagged 5F7—The 5F7 coding sequence was recloned into a *Pichiapastoris* compatible expression vector and provided with a C-terminal cysteine. The resulting Nb format (5F7GGC) was produced in *Pichiapastoris* X-33 in a 2L fermentor (BiostatBplus, Sartorius) in complex medium and induced with MeOH at pH 5 and 30°C. The cell broth was first clarified via centrifugation and the cell free medium was filtered through a 0.22μm GP Express PLUS Membrane (Millipore, USA).

The batch of 5F7GGCNb used in the radiolabeled Nb experiments described herein was purified from *Pichiapastoris* supernatants at the Free University of Brussels. All purifications were carried out on AKTA purifier workstations (GE Healthcare). The Nb was captured from the medium using a Protein A affinity chromatography POROS Mab Capture A column (Applied Biosystems) eluted with 100mM glycine, pH2.6. The eluate was immediately neutralized with 1/10 v/v 1M Tris-HCl, pH 8.0. The Protein A eluate was pooled, filtered, and concentrated on a 5kDa cut-off Vivaspin HY, and then further purified via size exclusion chromatography and buffer exchanged to PBS on a Superdex 75 16/60 column (GE Healthcare). Sodium dodecyl sulfate polyacrylamide gel electrophoresis (SDS-PAGE) indicated the presence of two peaks corresponding to the monovalent form and a disulfide-bridged dimer. This material was finally sterile filtered through a 0.22μm membrane and stored at −20°C. The final concentration was 3.84 mg/ml.

2.3. Cells and culture conditions

The human breast carcinoma cell line BT474M1 was kindly provided by Dr. Timothy Clay, Department of Medicine, Duke University. It was derived from the BT474 cell line and was selected for its increased tumorigenicity [22]. BT474M1 cells were cultured in DMEM/F12 medium supplemented with 10% fetal calf serum (FCS), streptomycin (100 μg/ml), and penicillin (100 IU/ml)(Sigma Aldrich, USA). The cells were grown at 37°C in a humidified incubator containing 5% CO_2. The medium was exchanged every two days and the cells were sub-cultured by trypsinization (0.05% Trypsin-EDTA) when they were about 80% confluent.

2.4. Radioiodination of Nb

[^{125}I]I-Nb—A solution of 5F7GGCNb(96 μg; 3.84mg/ml) in PBS, pH 7.4, was added to a ½-dram vial coated with 10 μg Iodogen (Thermo Scientific, Rockford, IL, USA) followed by 1–7 μl of a solution of sodium [^{125}I]iodide(~11.1–92.5 MBq). The mixture was incubated at room temperature for 10 min with occasional shaking, and the labeled protein was isolated by gel filtration on a PD-10 column (GE Healthcare, Piscataway, NJ, USA) eluted with PBS.

[^{131}I]IB-Mal-D-GEEEK-Nb—5F7GGCNb was dialyzed overnight against 0.1 M phosphate buffer (PB), pH 8.0, containing 5mM EDTA. A solution of the dialyzed Nb (96 μg; 3.84mg/ml) was treated with 2-iminothiolane(4 mg/ml; 148 nmol)in 0.1M PB containing 5mM EDTA, pH 8.0. After 90 min incubation at room temperature, the Nb was isolated using a Micro-spin G-25 column (GE Healthcare, Piscataway, NJ, USA) that had been equilibrated with 0.1M PB containing 5mM EDTA, pH 7.0. The formation of two sulfhydryl groups per Nb was established by Ellman's assay. The above thiol-derivatized Nb at pH 7.0 was mixed with dry [^{131}I]IB-Mal-D-GEEEK(~7.4–59.2 MBq) and incubated at room temperature for 45 min with occasional shaking. The reaction was quenched by incubation with 10 μ liodoacetamide(100 mg/ml in PB/EDTA pH 7.0)for 15 min at room temperature. The labeled Nb was purified on a PD-10 column as described above. For determination of K_D, the Nb was also labeled using [^{125}I]IB-Mal-D-GEEEK.

2.5. Determination of protein-associated radioactivity and immunoreactivity evaluation

The protein-associated radioactivity of labeled 5F7GGCNb was determined in paired-label format by co-precipitation with 20% (w/v) trichloroacetic acid (TCA) as described elsewhere [19]. Protein-associated radioactivity also was determined by instant thin layer chromatography (ITLC) using glass microfiber sheets impregnated silica gelstrips (Varian, Lake Forest, CA, USA) developed with PBS, pH 7.4.

Radiolabeled Nbs were also analyzed by SDS-PAGE under non-reducing conditions. Briefly, 100 nCi of each labeled Nb was mixed with 10 μl of PBS and 20 μl of Laemmli buffer (BioRad, Hercules, CA, USA) and incubated at 95°C for 15 min. The incubates were cooled to room temperature, spun, and 10 μ leach of the supernatants was added to wells of Mini-PROTEAN TGX Any kD gels (BioRad, Hercules, CA, USA) and electrophoresis was run for 40 min at 140 V. Radioactivity on dried gels was visualized using a Storage Phosphor System Cyclone Plusphosphor imager (Perkin-Elmer Life and Analytical Sciences, Downers Grove, IL, USA) and analyzed using OptiQuant version 5.0 software provided by the manufacturer.

The immunoreactive fraction of the labeled Nbs was determined in paired-label format using magnetic beads coated with recombinant human ErbB2/HER2 Fc chimera (R&D Systems, Minneapolis, MN, USA) and analyzed according to the Lindmo method [23]. Magnetic beads coated with the extracellular domain of ErbB2/HER2 were prepared as described previously[17]. Briefly, recombinant human ErbB2/HER2 was first biotinylated using a Chroma Link Biotin Protein Labeling Kit (SoluLink, San Diego, CA, USA) using the manufacturer's protocol, and coupled to streptavidin-coated magnetic beads (PureBiotech, Middlesex, NJ, USA) at a 1:1 ratio at room temperature for 1 h. Beads were rinsed with 115 mMPB, pH 7.4, containing 0.05% Brij 35, 0.05% BSA and 0.05% sodium azide to remove unbound protein. After resuspension in 230 μl of the same buffer, beads were stored at 4°C. Control beads were prepared in the same way except that biotinylated BSA was conjugated to the beads.

2.6. Evaluation of affinity

The binding affinities of [^{125}I]I-Nb and [^{125}I]IB-Mal-D-GEEEK-Nb to the HER2-expressing BT474M1 cell line was determined. The cells were plated in 24-well plates at a density of 8×104 cells/well 24 h prior to the experiment. On the day of the experiment, the plates were brought to 4°C for 30 min prior to incubation in triplicate with increasing concentrations of the radiolabeled Nb (0.1–300nM). To determine non-specific binding, a parallel assay was performed in which cells were co-incubated with a100-fold excess of trastuzumab. Cells were incubated for 2h at 4°C, the medium containing unbound radioactivity was removed, and the cells were washed twice with cold PBS. Finally, the cells were solubilized by treatment with 1 N NaOH(0.5 ml) at 37°C for 10 min. Cell-associated ^{125}I was determined using the automated gamma counter. The experiment was repeated two times. The data were fitted using GraphPad Prism software to determine K_D values.

2.7. Paired-label internalization assay

The percentage of uptake and internalization of radioiodinated Nbs were determined in a paired-label experiment using the BT474M1 cell line. Cells were seeded 24 h prior to the experiment in 6-well plates at a density of 80×104 cells/well. On the day of the experiment, the plates were placed at 4°C for 30 min and then incubated with 100 ng of both labeled Nbs at 4°C for 1 h. Non-specific uptake was determined by co-incubation with a 1000-fold excess of trastuzumab. The internalization and cellular processing assay was preformed

three times, with triplicate samples for each time point, as described in previous publications [17,24].

2.8. Paired-label biodistribution studies

Animal studies were performed under guidelines established by the Duke University Institutional Animal Care and Use Committee. Female 10–12 week old NOD. CB17-*Prkdc*^{scid}/J mice (Jackson Labs. Bar Harbor, ME, USA) were implanted with 60-day continuous release 17-β-estradiol pellets (0.72 mg, Innovative Research of America; Sarasota, FL, USA) on their back 2 days prior to tumor implantation. BT474M1 tumor cells (5×10^6) in 50% Matrigel (BD Biosciences, Bedford, MA, USA) were injected subcutaneously into the right flank and tumors were allowed to develop until they reached a volume of 350–500 mm^3.

Mice were injected via the tail vein with about 150kBq of both[^{125}I]I-Nb (0.2 μg) and [^{131}I]IB-Mal-D-GEEEK-Nb (0.4 μg) in 100 μl PBS. Groups of 5 animals were killed by an overdose of isofluorane and dissected at 1, 2, 4, 8 and 24 h. Organs of interest and blood were collected, blotted dry, weighed, and counted, together with injection standards, in an automated dual-channel gamma counter for ^{125}I and ^{131}I radioactivity. Results were expressed as percentage of injected dose per gram of tissue (%ID/g). To determine the specificity of uptake, 5 mice were injected with a 1500-fold molar excess of trastuzumab 24 h prior to radioiodinated Nb administration. Two hours later, the mice were killed and tissue distribution determined as described above. Difference in tissue radioactivity levels of the two labeled Nbs were analyzed with a paired 2-tailed Student *t*-test using the Microsoft Excel program, with $P< 0.05$ considered to represent a significant difference.

2.9 Analysis of radioactivity in the urine

The nature of labeled molecules present in the urine after intravenous injection of the two labeled Nb preparations was evaluated in Balb/c mice. Groups of 5 mice were injected with either 2.78MBq (4 μg) of [^{125}I]I-Nbor 3.33MBq (5 μg) of [^{125}I]IB-Mal-D-GEEEK-Nb and urine samples were collected 1 h later. Urine was filtered through a 0.22 μm filter (Millipore, USA) before analysis. The fraction of radioiodine activity present in the urine as intact Nb and low molecular weight catabolites was analyzed by ITLC and gel electrophoresis using Mini-PROTEAN Tris-Tricine Precast Gels (BioRad, Hercules, CA, USA) as described above.

3. Results

3.1. Generation and characterization of anti-HER2 Nb 5F7

To obtain Nb specific for HER2, phage Nb repertoires were synthesized from peripheral blood lymphocytes from llamas immunized with HER2 over-expressing SKBR3 tumor cells. After panning to immobilized ErbB2/Fc chimera followed by competitive elution with trastuzumab, single clones were screened as periplasmic extracts by an enzyme-linked immunosorbent assay for HER2 reactivity. Approximately 90% of the clones tested were found to bind HER2 and flow cytometry analysis confirmed the specific character of HER2 recognition by the purified Nbs (data not shown). Next, the ability of the Nbs to compete with the binding of trastuzumab to HER2 was assessed in a FMAT based whole cell homogenous assay and resulted in a final panel of several clones which showed good competition with trastuzumab for HER2 interaction (Fig. 1). Nb 5F7 was selected from this panel for further analysis. Surface plasmon resonance analysis was utilized to determine the kinetic parameters for Nb binding to HER2, which indicated that 5F7 Nb displays sub-nanomolar dissociation constant, K_D, of 0.51 nM ($k_a = 1.054\times10^6 M^{-1}s^{-1}$; $k_d = 5.381\times10^{-4}s^{-1}$).

3.2 Radiolabeling of Nb

The radioiodination of 5F7GGCNb by a direct method, Iodogen, gave an average radiochemical yield of 83.6±5.0% (n=10). The tin precursor TB-Mal-D-GEEEK was radioiodinated to [^{131}I]IB-Mal-D-GEEEK in 91.2±4.4% (n=25) radiochemical yield and in more than 99% radiochemical purity after HPLC purification. The efficiency for conjugation of [^{131}I]IB-Mal-D-GEEEK to thiolated 5F7GGCNb was 59.6±9.4% (n = 15), comparable to results observed previously with larger proteins [19,20,25]. The specific activity of the directly radioiodinated Nb preparations ranged from 37 to 910 MBq/mg, whereas for [^{131}I]IB-Mal-D-GEEEK-Nb, the range was 15 to 352MBq/mg. Co-precipitation of the labeled Nb with human serum albumin using 20% TCA indicated that 88.5±4.9% and 95.1±2.5% of the radioactivity was protein-associated for [^{125}I]I-Nb and [^{131}I]IB-Mal-D-GEEEK-Nb, respectively. Protein-associated radioactivity, determined by ITLC, was 89.5±4.3% and 91.3±4.4% for [^{125}I]I-Nb and [^{131}I]IB-Mal-D-GEEEK, respectively. The immunoreactive fraction was 60.5±4.2% and 75.3±19.6% for [^{125}I]I-Nb and [^{131}I]IB-Mal-D-GEEEK-Nb, respectively. The Nb used in these studies contains a carboxy-terminal cysteine, and as such is an equilibrium mixture of monomeric and dimeric forms. No reducing agents, like dithiothreitolor *tris*(2-carboxyethyl)phosphine, were used prior to labeling. The results from SDS-PAGE, analyzed by phosphor imaging, showed that the Nb labeled using Iodogen consisted of 63.4±0.6% monomer (~13kDa), and 36.6±0.6% dimer (~26kDa)(Fig. 2). For Nb radioiodinated using [^{131}I]IB-Mal-D-GEEEK, monomer and dimer accounted for 69.0±5.7% and 31.0±5.7%, respectively. The dissociation constants (K_D) for the binding of radioiodinated Nb to the BT474M1 human breast carcinoma cell line were 1.8±0.6 nM and 3.2±1.0 nM for [^{125}I]I-Nb and [^{131}I]IB-Mal-D-GEEEK-Nb, respectively (Fig. 3).

3.3 Paired-label internalization of labeled Nbs

The *in vitro* paired-label internalization studies using the BT474M1 cell line revealed that the cellular retention of [^{131}I]IB-Mal-D-GEEEK-Nb was fairly constant over 24 h (1 h: 56.9±4.1%; 24 h: 58.3±4.6%). On the other hand, the retention of [^{125}I]I-Nb steadily decreased with time, from 61.4±4.3% at 1 h to 32.4±2.0% at 24 h. Uptake at all-time points was reduced to background levels for both tracers when the cells were co-incubated with 1000-fold excess of trastuzumab, confirming that labeled Nb uptake reflected the HER2 expression of this cell line. Figure 4 depicts the percentage of initially bound radioactivity that was specifically internalized, membrane-bound, and released into the cell culture supernatants for both labeled Nbs. The internalized radioactivity from both labeled Nbs was similar until 6h; by 24 h, [^{131}I]IB-Mal-D-GEEEK-Nb demonstrated about a 2-fold advantage in intracellular retention. The membrane-bound radioactivity for both tracers was considerably lower than internalized counts over the course of the assay. Cell culture supernatants were analyzed to determine the fraction of radioactivity that was no longer protein-associated;. The fraction of radioactivity associated with small molecular weight catabolites (*i.e.* TCA-soluble radioactivity) for[^{125}I]I-Nb increased from 6.3±0.8% at 1 h to 52.9±1.9% at 24 h. On the other hand, these values were considerably lower for [^{131}I]IB-Mal-D-GEEEK-Nb (3.8±2.3% at 1 h to 17.5±4.2% at 24 h).

3.4 Biodistribution and urine analysis

The tissue distribution of [^{125}I]I-Nb and [^{131}I]IB-Mal-D-GEEEK-Nb in mice bearing subcutaneous BT474M1 xenografts 2 h post injection, in comparison with mice group pretreated with trastuzumab, is shown in Table 1. Trastuzumab pretreatment decreased tumor uptake of [^{125}I]I-Nb and [^{131}I]IB-Mal-D-GEEEK-Nb to 33% and 20% of control values, respectively, confirming HER2 specific uptake for both labeled Nbs. Tumor uptake for Nb labeled using [^{131}I]IB-Mal-D-GEEEK was significantly (P<0.05) higher than that for Nb labeled using ^{125}I with Iodogen at all time points (Fig. 5). For example, the uptake

of ^{131}I in BT474M1 xenografts was 1.5-fold (4.7±0.6% vs. 2.9±0.2%) and 3-fold (3.6±1.2% vs. 1.2±0.3%) higher than that of ^{125}I at 8 and 24 h, respectively. Compared to [^{125}I]I-Nb, [^{131}I]IB-Mal-D-GEEEK-Nb exhibited lower uptake in most normal tissues except kidneys at all-time points. For example, in the lungs and muscle, the uptake of ^{131}I was about 3- to 4-fold lower than that of ^{125}I from 1 to 8 h., while more than 5-fold lower activity levels were observed in the blood, reflecting the very fast clearance of [^{131}I]IB-Mal-D-GEEEK-Nb. On the other hand, 9- to 28-fold ($P< 0.002$) higher kidney levels were seen for [^{131}I]IB-Mal-D-GEEEK-Nb at all-time points (Fig. 5). The thyroid uptake of ^{131}I was 20–100-fold lower than that of ^{125}I, indicating a considerably lower degree of deiodination for [^{131}I]IB-Mal-D-GEEEK-Nb *in vivo* (Fig. 6). Consistent with this, uptake of ^{131}I in the stomach, another tissue known to take up iodide avidly [26,27], also was significantly lower than that for ^{125}I. Except in the kidneys, tumor-to-normal tissue ratios for [^{131}I]IB-Mal-D-GEEEK-Nb generally were higher than those for [^{125}I]I-Nb (Fig. 7). For example, tumor-to-liver ratios for [^{131}I]IB-Mal-D-GEEEK-Nb were about 1.5 times higher than those for [^{125}I]I-Nb with the differences statistically significant ($P= 0.05$) at all-time points. The tumor-to-blood ratios for [^{131}I]IB-Mal-D-GEEEK-Nb(2.1±0.7, 4.8±0.8, 8.8±4.2, 16.2±5.7 and 35.9±11.4, respectively) were significantly ($P< 0.05$) higher than those for [^{125}I]I-Nb(0.4±0.1, 0.5±0.1, 0.6±0.1, 0.7±0.1 and 0.8±0.2, respectively)at 1, 2, 4, 8 and 24 h. Analysis of urine samples obtained from normal mice 1 h after labeled Nb administration indicated that the fraction of activity associated with intact Nb was significantly higher ($P< 0.05$) for [^{131}I]IB-Mal-D-GEEEK-Nb(46 ± 11%) compared with [^{125}I]I-Nb (20.6 ± 4.1%)..

4. Discussion

The importance of trastuzumab in the current management of patients with breast cancer provided motivation for developing a Nb specific for HER2. The smaller size of Nbs could be advantageous for diagnostic and therapeutic applications because it facilitates tumor penetration and recognition of hidden epitopes that are less accessible to intact mAbs [28]. An additional consequence of this property is their rapid normal tissue clearance, making them compatible for use with short half-life radionuclides such as ^{68}Ga and ^{18}F for PET imaging and ^{211}At for targeted radiotherapy.

In previous studies, we demonstrated the effectiveness of IB-Mal-D-GEEEK, consisting of a D-peptide core, for labeling internalizing biomolecules [19,20]. Labeling an anti-EGFRvIIImAb L8A4 and a 105 kDa double mutant single-chain Fv-Fc fragment (scFv-Fc DM) with IB-Mal-D-GEEEK increased tumor retention of radioactivity compared to directly labeled protein. We embarked on the current study to evaluate the potential advantages of combining the targeting properties of Nbs with the residualizing capability of the IB-Mal-D-GEEEK prosthetic group. The 5F7GGCN blabeled with [^{131}I]IB-Mal-D-GEEEK possessed high-affinity binding to HER2-expressing BT474M1 cells, with a K_D similar to that for Nb labeled using Iodogen.

Intracellular retention of radioactivity in BT474M1 cells was similar for both labeled Nbs up to 6 h; however, at 24 h, intracellular retention was about twofold higher for [^{131}I]IB-Mal-D-GEEEK-Nb and TCA-soluble cell culture supernatant counts were concomitantly lower. These results suggest that the residualizing effect of the D-peptide prosthetic group was only realized at later time points, which is in marked contrast to the behavior observed previously when IB-Mal-D-GEEEK was utilized for labeling an intact mAb L8A4[19] and a105-kDa scFv-Fc DM fragment [20]. A slower rate of internalization for the Nb could explain this behavior; however, this is not consistent with the observation of more than 50% cellular internalization of Nb within 1 h. Another possibility is a slower rate of Nb transport into protease-rich lysosomes, perhaps reflecting the lack of Fc region in the Nb or the nature of the receptor-labeled protein complex formed on the cell surface.

Results from the tissue distribution studies also demonstrated potential advantages for using [^{131}I]IB-Mal-D-GEEEK to label this Nb. This likely reflects not only the residualizing property of this prosthetic group, but also its low susceptibility to deiodination, indicated by very low uptake in thyroid and stomach. It is worth noting that the tumor uptake of the [^{131}I]IB-Mal-D-GEEEK anti-HER2 Nb conjugate was higher than that seen for an scFv-Fc DM derived from trastuzumab and labeled with the same prosthetic group[20]. Moreover, the tumor uptake of [^{131}I]IB-Mal-D-GEEEK-Nb also was equal to that reported for another HER2-reactive Nb,7C12, labeled with ^{99m}Tc [29].

Uptake of[^{131}I]IB-Mal-D-GEEEK-Nb was lower than that of [^{125}I]I-Nb in almost all normal tissues; however, substantially higher kidney uptake was seen for this conjugate. High levels of kidney uptake generally are observed for peptides and proteins with molecular weights<60 kDa, reflecting their renal clearance and tubular reabsorption [30]. Similar behavior has been reported previously for anti-EGFRNbs[31,32], other anti-HER2Nbs[29], and anti-HER2 affibodies[33,34]. However, renal activity levels observed for [^{131}I]IB-Mal-D-GEEEK-Nb were about 10 to 25 times higher than those for co-administered[^{125}I]I-Nb. With regard to properties of IB-Mal-D-GEEEK that could account for this behavior, in a study with ^{99m}Tc-labeled $Z_{HER2:342}$ affibody modified with different mercaptoacetyl-peptides, exchange of three glycines with glutamic acids increased kidney uptake by a factor of 10 [34]. The IB-Mal-D-GEEEK prosthetic group also contains three glutamic acids, albeitas D-enantiomers. Small proteins such as Nbs excreted via kidneys are partly reabsorbed in the proximal tubular cells, with reabsorption dependent on several processes including EAAT3 transporters, and megalin and cubilin receptors. EAAT3 is the high-affinity transporter for anionic amino acids, is highly expressed in kidneys and is the major transporter for L-glutamic acid [35,36]. The degree to which the D-glutamic acids present in IB-Mal-D-GEEEK could act as a substrate for this transporter is currently unknown. Moreover, it is important to note that the effects of glutamic acid residues on kidney uptake are difficult to predict because introduction of this negatively charged amino acid has been reported to both significantly reduce [37,38]and increase [39,40] activity levels in the kidney.

Although the lower activity levels observed in most normal tissues for Nb labeled using IB-Mal-D-GEEEK should facilitate imaging of metastases in these sites, detection of lesions in or near the kidneys would be problematic and for targeted radiotherapy, nephrotoxicity could be an issue. A tactic that is often used to reduce renal uptake of radiopharmaceuticals is the pre-administration of positively charged lysine or arginine [18,41]; however, this may not work when the negatively charged [^{131}I]IB-Mal-D-GEEEK prosthetic group is employed. Competitive inhibition of renal transport mechanisms also can be achieved through co-infusion of gel of usine (succinylated gelatin), albumin fragments or albumin-derived peptides, which has been shown to significantly reduce kidney retention of radiolabeled peptides [30]. For example, co-injection of gel of usine and lysine with an anti-EGFR ^{99m}Tc-7C12 Nb not only reduced renal retention by 45%, but also improved tumor uptake [28]. Moreover, the same strategy has been used successfully in patients treated with ^{90}Y-DOTATOC or ^{177}Lu-DOTATATE [30].

5. Conclusions

A Nb has been generated that binds with high affinity to HER2 and is internalized by breast carcinoma cells expressing these receptors. Radioiodination of 5F7GGC Nb using the [^{131}I]IB-Mal-D-GEEEK prosthetic group resulted in better tumor targeting properties both *in vitro* and *in vivo* compared with Nb labeled via Iodogen. Tumor-to-normal tissue ratios generally were higher with [^{131}I]IB-Mal-D-GEEEK-Nb except in the kidneys where substantially higher radioactivity levels were observed. We are currently exploring

alternative residualizing labeling strategies and tactics for reducing renal retention in order to better exploit the potential of this Nb for imaging, and possibly, treatment of HER2-expressing malignancies.

Acknowledgments

This work was supported in part by Grants CA42324, CA154291, and CA14236 from the National Institutes of Health. The authors wish to thank to Xiao-Guang Zhao for excellent technical assistance. We also wish to thank Dr. Timothy Clay, Department of Medicine, Duke University Medical Center, for providing the BT474M1 breast carcinoma cell line. Tony Lahoutte is a senior clinical investigator of the Research Foundation Flanders (FWO).

References

1. Yarden Y, Sliwkowski MX. Untangling the ErbB signalling network. Nat Rev Mol Cell Biol. 2001; 2:127–37. [PubMed: 11252954]
2. Ménard S, Casalini P, Campiglio M, Pupa S, Agresti R, Tagliabue E. HER2 overexpression in various tumor types, focusing on its relationship to the development of invasive breast cancer. Ann On col. 2001; 12:S15–9.
3. Scholl S, Beuzeboc P, Pouillart P. Targeting HER2 in other tumor types. Ann Oncol. 2001; 12:S81–7. [PubMed: 11521727]
4. Hede K. Gastric cancer: trastuzumab trial results spur search for other targets. J Natl Cancer Inst. 2009; 101:1306–7. [PubMed: 19755679]
5. Metro G, Mottolese M, Fabi A. HER-2-positive metastatic breast cancer: trastuzumab and beyond. Expert Opin Pharmacother. 2008; 9:2583–601. [PubMed: 18803447]
6. Santin AD, Bellone S, Roman JJ, McKenney JK, Pecorelli S. Trastuzumab treatment in patients with advanced or recurrent endometrial carcinoma overexpressing HER2/neu. Int J Gynecol Obstet. 2008; 102:128–31.
7. Kakar S, Puangsuvan N, Stevens JM, Serenas R, Mangan G, Sahai S, et al. HER-2/neu assessment in breast cancer by immunohistochemistry and fluorescence in situ hybridization: comparison of results and correlation with survival. Mol Diagn. 2000; 5:199–207. [PubMed: 11070154]
8. Harmsen MM, De Haard HJ. Properties, production, and applications of camelid single-domain antibody fragments. Appl Microbiol Biotechnol. 2007; 77:13–22. [PubMed: 17704915]
9. Revets H, De Baetselier P, Muyldermans S. Nanobodies as novel agents for cancer therapy. Expert Opin Biol Ther. 2005; 5:111–124. [PubMed: 15709914]
10. Huang L, Muyldermans S, Saerens D. Nanobodies®: proficient tools in diagnostics. Expert Rev Mol Diagn. 2010; 10:777–85. [PubMed: 20843201]
11. Rahbarizadeh F, Ahmadvand D, Sharifzadeh Z. Nanobody; an old concept and new vehicle for immunotargeting. Immunological Investigations. 2011; 40:299–338. [PubMed: 21244216]
12. Geissler F, Anderson SK, Press O. Intracellular catabolism of radiolabeled anti-CD3 antibodies by leukemic T cells. Cell Immunol. 1991; 137:96–110. [PubMed: 1832089]
13. Reist CJ, Garg PK, Alston KL, Bigner DD, Zalutsky MR. Radioiodination of internalizing monoclonal antibodies using N-succinimidyl 5-iodo-3-pyridinecarboxylate. Cancer Res. 1996; 56:4970–7. [PubMed: 8895752]
14. Reist CJ, Archer GE, Wikstrand CJ, Bigner DD, Zalutsky MR. Improved targeting of an anti-epidermal growth factor receptor variant III monoclonal antibody in tumor xenografts after labeling using N-succinimidyl 5-iodo-3-pyridinecarboxylate. Cancer Res. 1997; 57:1510–5. [PubMed: 9108453]
15. Vaidyanathan G, Affleck DJ, Bigner DD, Zalutsky MR. Improved xenograft targeting of tumor-specific anti-epidermal growth factor receptor variant III antibody labeled using N-succinimidyl 4-guanidinomethyl-3-iodobenzoate. Nucl Med Biol. 2002; 29:1–11. [PubMed: 11786270]
16. Shankar S, Vaidyanathan G, Affleck DJ, Peixoto K, Bigner DD, Zalutsky MR. Evaluation of an internalizing monoclonal antibody labeled using N-succinimidyl 3-[^{131}I]iodo-4-phosphonomethylbenzoate ([^{131}I]SIPMB), a negatively charged substituent bearing acylation agent. Nucl Med Biol. 2004; 31:909–19. [PubMed: 15464393]

17. Foulon CF, Reist CJ, Bigner DD, Zalutsky MR. Radioiodination via D-amino acid peptide enhances cellular retention and tumor xenograft targeting of an internalizing anti-epidermal growth factor receptor variant III monoclonal antibody. Cancer Res. 2000; 60:4453–60. [PubMed: 10969792]
18. Foulon CF, Welsh PC, Bigner DD, Zalutsky MR. Positively charged templates for labeling internalizing antibodies: comparison of N-succinimidyl 5-iodo-3-pyridinecarboxylate and the D-amino acid peptide KRYRR. Nucl Med Biol. 2001; 28:769–77. [PubMed: 11578897]
19. Vaidyanathan G, Alston KL, Bigner DD, Zalutsky MR. N^{ε}-(3-[*I]Iodobenzoyl)-Lys^5-N^{α}-maleimido-Gly^1-GEEEK ([*I]IB-Mal-D-G EEEK): a radioiodinated prosthetic group containing negatively charged D-glutamates for labeling internalizing monoclonal antibodies. Bioconjugate Chem. 2006; 17:1085–92.
20. Vaidyanathan G, Jestin E, Olafsen T, Wu AM, Zalutsky MR. Evaluation of an anti-p185^{HER2} (scFv-C_H2-C_H3)$_2$ fragment following radioiodination using two different residualizing labels: SGMIB and IB-Mal-D-GEEEK. Nucl Med Biol. 2009; 36:671–80. [PubMed: 19647173]
21. Roovers RC, Laeremans T, Huang L, De Taeye S, Verkleij AJ, Revets H, et al. Efficient inhibition of EGFR signalling and of tumour growth by antagonistic anti-EGFR Nanobodies. Cancer Immunol Immun other. 2007; 56:303–317.
22. Yu Z, Xia W, Wang H-Y, Wang S-C, Pan Y, Kwong KY, et al. Antitumor activity of an Etsprotein, PEA3, in breast cancer cell lines MDA-MB-361DYT2 and BT474M1. Mol Carcinog. 2006; 45:667–75. [PubMed: 16652376]
23. Lindmo T, Boven E, Cuttitta F, Fedorko J, Bunn PA. Determination of the immunoreactive fraction of radiolabeled monoclonal antibodies by linear extrapolation to binding at infinite antigen excess. J Immunol Methods. 1984; 72:77–89. [PubMed: 6086763]
24. Shankar S, Vaidyanathan G, Affleck D, Welsh PC, Zalutsky MR. N-succinimidyl 3-[^{131}I]Iodo-4-phosphonomethylbenzoate ([^{131}I]SIPMB), a negatively charged substituent-bearing acylation agent for the radioiodination of peptides and mAbs. Bioconjugate Chem. 2003; 14:331.
25. Mume E, Orlova A, Larsson B, Nilsson A-S, Nilsson F, Sjöberg S, et al. Evaluation of ((4-hydroxyphenyl)ethyl)maleimide for site-specific radiobromination of anti-HER2 affibody. Bioconjugate Chem. 2005; 16:1547–55.
26. Zalutsky MR, Colcher D, Kaplan WD, Kufe DW. Radioiodinated B6. 2 monoclonal antibody: further characterization of a potential radiopharmaceutical for the identification of breast tumors. Int J Nucl Med Biol. 1985; 12:227–33. [PubMed: 3905666]
27. Freitas JE, Gross MD, Ripley S, Shapiro S. Radionuclide diagnosis and therapy of thyroid cancer: current status report. Semin Nucl Med. 1985; 15:106–31. [PubMed: 2988129]
28. Gainkam LOT, Caveliers V, Devoogdt N, Vanhove C, Xavier C, Boerman O, et al. Localization, mechanism and reduction of renal retention of technetium-99m labeled epidermal growth factor receptor-specific Nanobody in mice. Contrast Media Mol Imaging. 2011; 6:85–92. [PubMed: 20936711]
29. Vaneycken I, Devoogdt N, Van Gassen N, Vincke C, Xavier C, Wernery U, et al. Preclinical screening of anti-HER2 Nanobodies for molecular imaging of breast cancer. FASEB J. 2011; 25:2433–46. [PubMed: 21478264]
30. Vegt E, De Jong M, Wetzels JFM, Masereeuw R, Melis M, Oyen WJG, et al. Renal toxicity of radiolabeled peptides and antibody fragments: mechanisms, impact on radionuclide therapy, and strategies for prevention. J Nucl Med. 2010; 51:1049–58. [PubMed: 20554737]
31. Gainkam LOT, Huang L, Caveliers V, Keyaerts M, Hernot S, Vaneycken I, et al. Comparison of the biodistribution and tumor targeting of two ^{99m}Tc-labeled anti-EGFR Nanobodies in mice, using pinhole SPECT/Micro-CT. J Nucl Med. 2008; 49:788–95. [PubMed: 18413403]
32. Huang L, Gainkam LOT, Caveliers V, Vanhove C, Keyaerts M, De Baetselier P, et al. SPECT imaging with ^{99m}Tc-labeled EGFR-specific Nanobody for in vivo monitoring of EGFR expression. Mol Imaging Biol. 2008; 10:167–75. [PubMed: 18297364]
33. Tran T, Engfeldt T, Orlova A, Widström C, Bruskin A, Tolmachev V, et al. In vivo evaluation of cysteine-based chelators for attachment of ^{99m}Tc to tumor-targeting Affibody molecules. Bioconjugate Chem. 2007; 18:549–58.

34. Tran T, Engfeldt T, Orlova A, Sandström M, Feldwisch J, Abrahmsén L, et al. ^{99m}Tc-maEEE-$Z_{HER2:342}$, an Affibody molecule-based tracer for the detection of HER2 expression in malignant tumors. Bioconjugate Chem. 2007; 18:1956–64.
35. Verrey F, Ristic Z, Romeo E, Ramadan T, Makrides V, Dave MH, et al. Novel renal amino acid transporters. Annu Rev Physiol. 2005; 67:557–72. [PubMed: 15709970]
36. Rexhepaj R, Grahammer F, Völkl H, Remy C, Wagner CA, Sandulache D, et al. Reduced intestinal and renal amino acid transport in PDK1 hypomorphic mice. FASEB J. 2006; 20:2214–22. [PubMed: 17077298]
37. Béhé M, Kluge G, Becker W, Gotthardt M, Behr TM. Use of polyglutamic acids to reduce uptake of radiometal-labeled minigastrin in the kidneys. J Nucl Med. 2005; 46:1012–15. [PubMed: 15937313]
38. Miao Y, Fisher DR, Quinn TP. Reducing renal uptake of ^{90}Y- and ^{177}Lu-labeled alpha-melanocyte stimulating hormone peptide analogues. Nucl Med Biol. 2006; 33:723–33. [PubMed: 16934691]
39. Ekblad T, Tran T, Orlova A, Widström C, Feldwisch J, Abrahmsén L, et al. Development and preclinical characterisation of ^{99m}Tc-labelled Affibody molecules with reduced renal uptake. Eur J Nucl Med Mol Imaging. 2008; 35:2245–55. [PubMed: 18594815]
40. Mather SJ, McKenzie AJ, Sosabowski JK, Morris TM, Ellison D, Watson SA. Selection of radiolabeled gastrin analogs for peptide receptor-targeted radionuclide therapy. J Nucl Med. 2007; 48:615–22. [PubMed: 17401100]
41. Behr TM, Becker WS, Sharkey RM, Juweid ME, Dunn RM, Bair H-J, et al. Reduction of renal uptake of monoclonal antibody fragments by amino acid infusion. J Nucl Med. 1996; 37:829–33. [PubMed: 8965154]

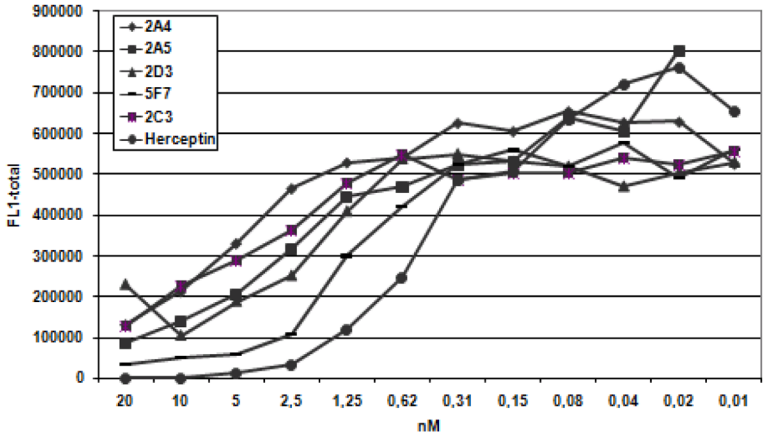

Fig. 1.

Herceptin®-competitive FMAT. HER2 binding Nanobodies were tested for their ability to block the binding of Herceptin® to HER2-overexpressing SKBR3 cells. All tested Nanobodies compete with binding of Herceptin® to SKBR3 cells in a dose-dependent manner.

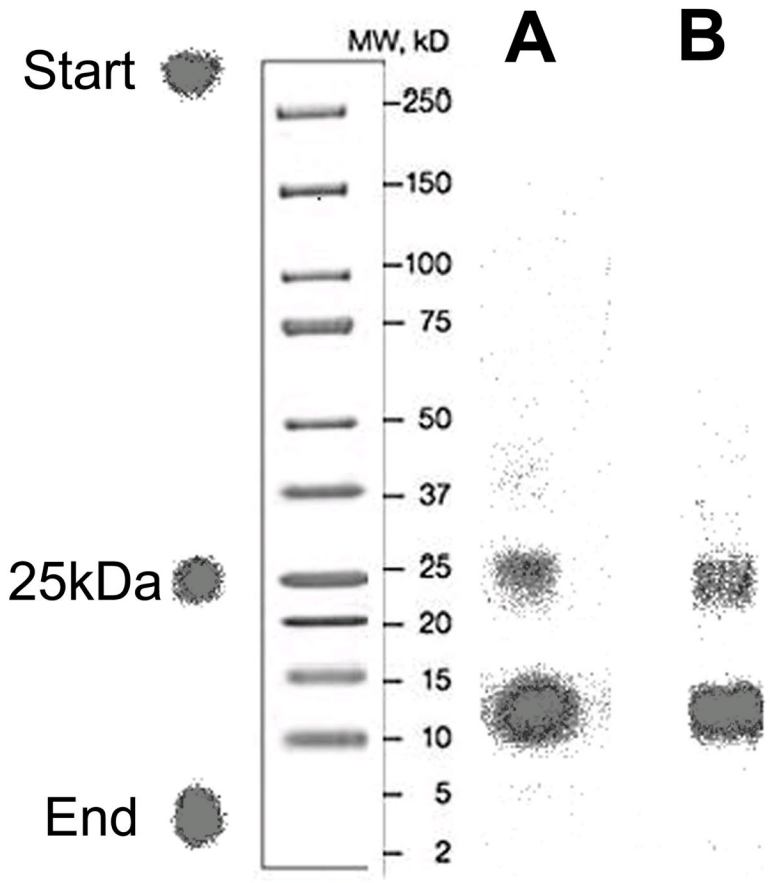

Fig. 2.
Non-reducing SDS-PAGE/phosphor image profiles of 5F7GGC Nb radioiodinated directly with ^{125}I using Iodogen (A) and with ^{131}I using [^{131}I]IB-Mal-D-GEEEK (B).

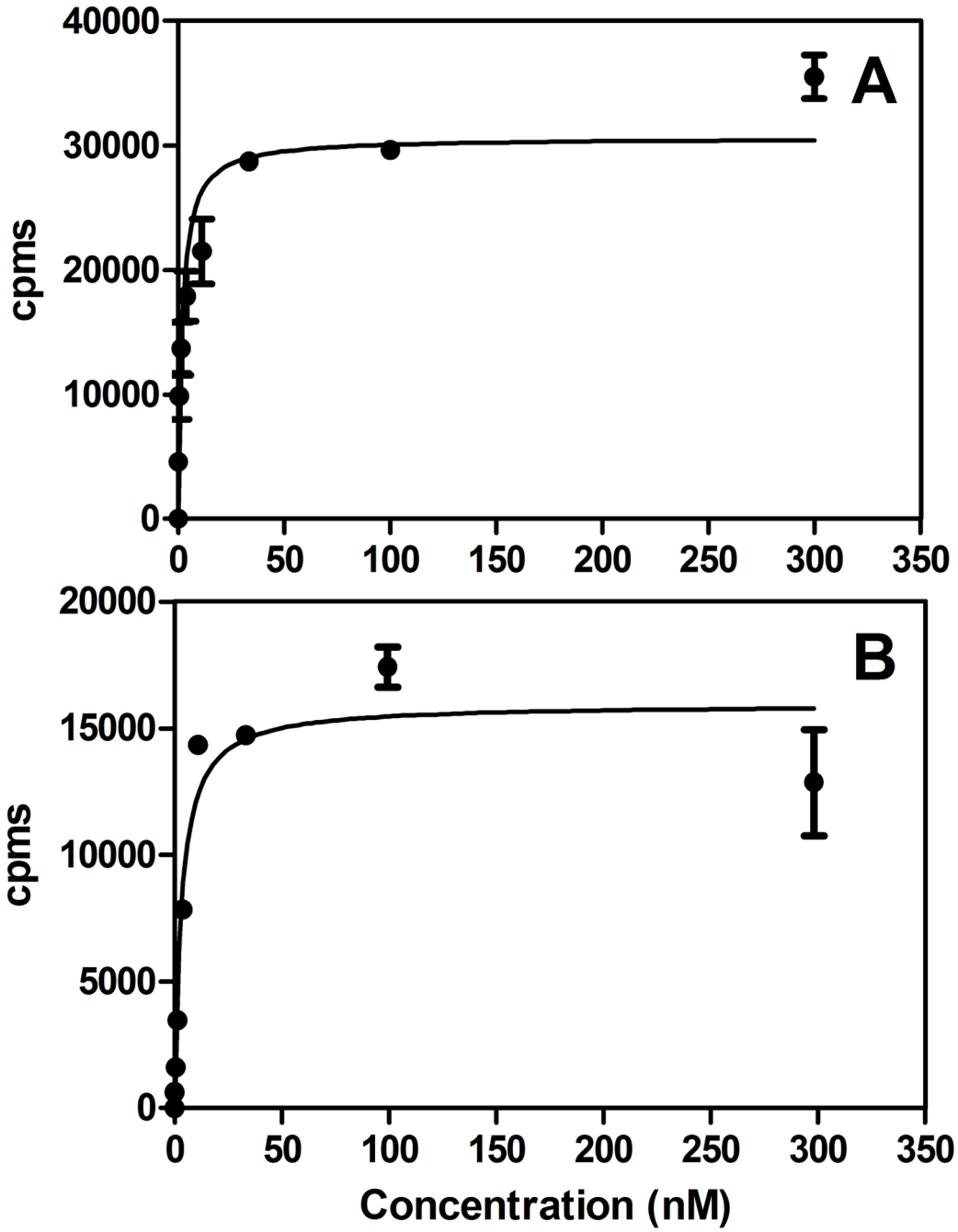

Fig. 3.
Representative cell binding affinity graph of [^{125}I]I-Nb(A) and [^{125}I]IB-Mal-D-GEEEK-Nb (B) using the human breast carcinoma cell line BT474M1.

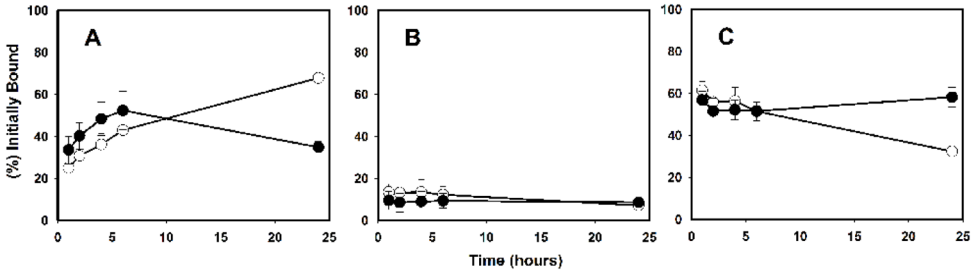

Fig. 4.

Paired-label internalization of [^{125}I]I-Nb (open circles) and [^{131}I]IB-Mal-D-GEEEK-Nb (closed circles) by BT474M1 cells. Data presented as the percentage of initially bound radioactivity (specific) that was in the cell culture supernatants (A), membrane-bound (B), and internalized (C) at various time points. Results are from three independent experiments, each time point in triplicate.

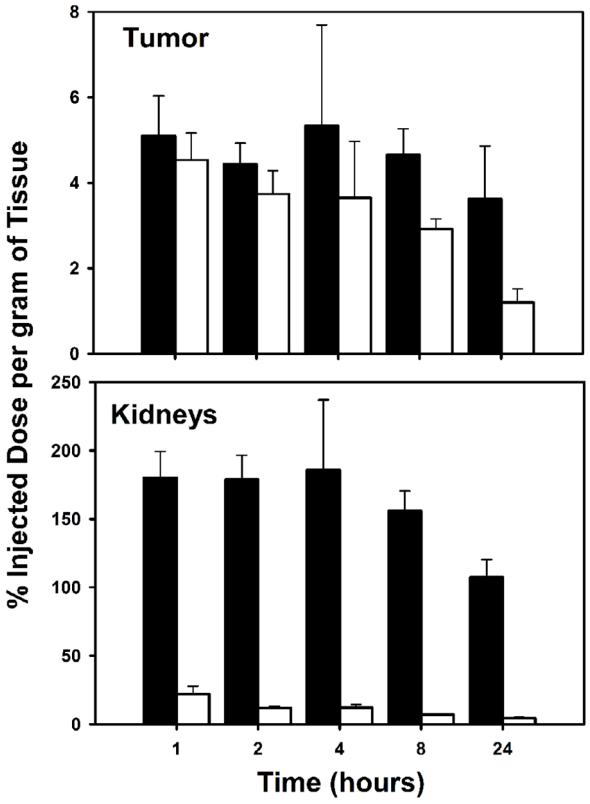

Fig. 5.

Paired-label tumor and kidneys uptake of radioiodine activity expressed as %ID/g in BT474M1 xenograft-bearing mice after the injection of [^{125}I]I-Nb (open bars) and [^{131}I]IB-Mal-D-GEEEK-Nb (filled bars).

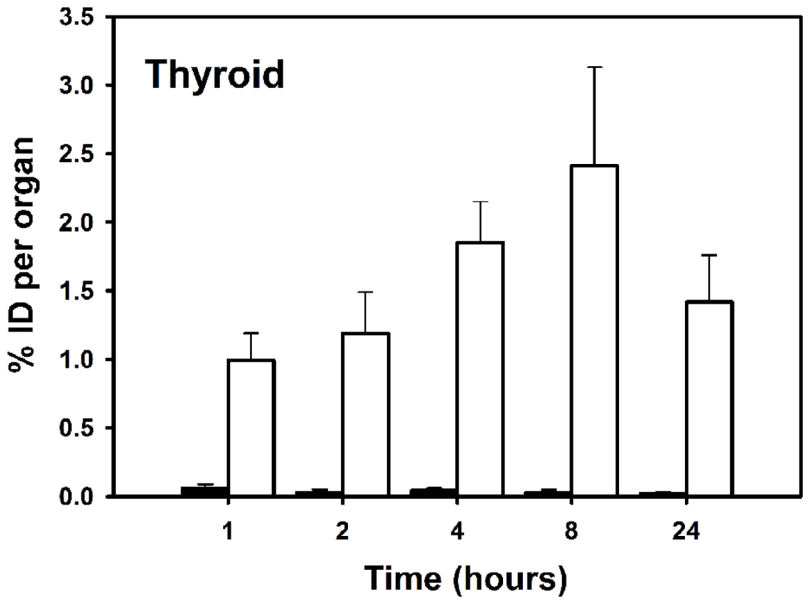

Fig. 6.

Uptake of radioiodine activity in mouse thyroid after administration of[^{125}I]I-Nb (open bars)and [^{131}I]IB-Mal-D-GEEEK-Nb (filled bars) in tumor-bearing mice.

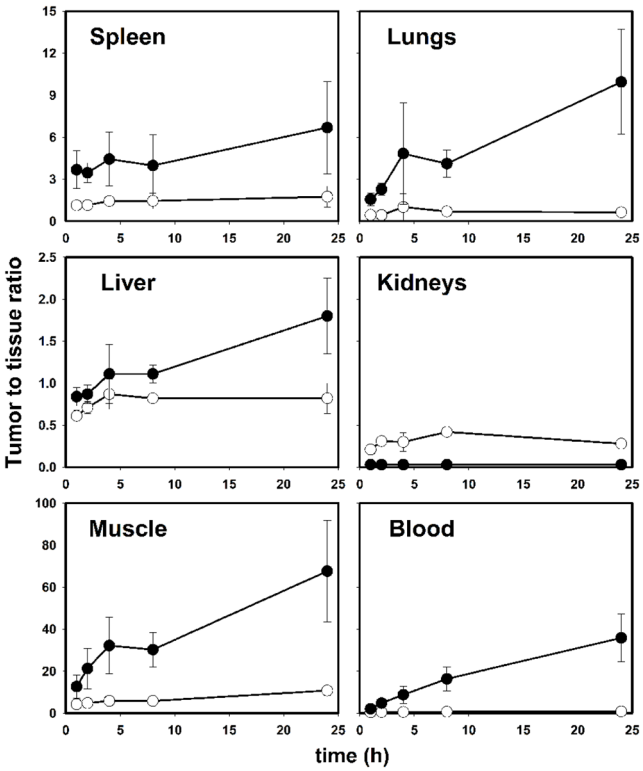

Fig. 7.
Tumor-to-tissue ratios obtained from the biodistribution of [^{125}I]I-Nb (open circles) and [^{131}I]IB-Mal-D-GEEEK-Nb (closed circles)in mice bearing BT474M1 xenografts.

Table 1

Paired-label biodistribution of [^{125}I]I-Nb and [^{131}I]IB-Mal-D-GEEEK-Nb 2 h after injection in mice bearing BT474M1 xenografts. Data for control mice and those pretreated with an excess of trastuzumab are shown.

Organ/Tissue	%ID/g [a]			
	Iodogen		*IB-Mal-$_D$-GEEEK*	
	Control	**Blocked**	**Control**	**Blocked**
Liver	5.26 ± 0.37	3.43 ± 0.23	5.15 ± 0.66	5.11 ± 0.29
Spleen	3.28 ± 0.43	2.09 ± 0.38	1.32 ± 0.26	1.39 ± 0.29
Lungs	8.53 ± 0.86	5.05 ± 1.43	2.01 ± 0.42	1.93 ± 0.39
Heart	2.51 ± 0.35	1.20 ± 0.07	0.48 ± 0.11	0.52 ± 0.06
Kidneys	12.06 ± 1.30	8.70 ± 3.19	179 ± 18	208± 17
Stomach	21.80 ± 4.38	17.56 ± 6.30	0.43 ± 0.09	0.53 ± 0.21
Small intestine	2.74 ± 0.33	1.66 ± 0.12	0.57 ± 0.19	0.46 ± 0.04
Large intestine	2.01 ± 0.18	1.38 ± 0.16	0.71 ± 0.10	0.90 ± 0.15
Thyroid	1.19 ± 0.30	1.05 ± 0.34	0.03 ± 0.02	0.05 ± 0.04
Muscle	0.81 ± 0.19	0.54 ± 0.07	0.24 ± 0.09	0.26 ± 0.04
Blood	7.71 ± 0.70	3.69 ± 0.29	0.94 ± 0.11	1.14 ± 0.15
Tumor	3.74 ± 0.54	1.25 ± 0.10	4.44 ± 0.48	0.87 ± 0.07
Bone	1.36 ± 0.18	0.73 ± 0.21	0.57 ± 0.15	0.48 ± 0.19
Brain	0.33 ± 0.04	0.20 ± 0.06	0.03 ± 0.01	0.04 ± 0.01

[a] Values are mean %ID/g ±SD (n=5) except for thyroid which %ID/organ is used.